articles

molecular pharmaceutics

Selectin Ligands Promote Ultrasound Contrast Agent Adhesion under Shear Flow

J. J. Rychak,[†] B. Li,[‡] S. T. Acton,[‡] A. Leppänen,[§,#] R. D. Cummings,[§] K. Ley,[†,||] and A. L. Klibanov*[,†,||,⊥]

University of Virginia Department of Biomedical Engineering, Charlottesville, Virginia, University of Virginia Department of Electrical and Computer Engineering, Charlottesville, Virginia, University of Oklahoma Health Sciences Center, Oklahoma City, Oklahoma, Department of Biological and Environmental Sciences, University of Helsinki, Helsinki, Finland, University of Virginia Robert M. Berne Cardiovascular Research Center, Charlottesville, Virginia, and University of Virginia Cardiovascular Division, Charlottesville, Virginia

Received May 11, 2006

Abstract: Contrast-enhanced ultrasound imaging has shown promise in the field of molecular imaging. This technique relies upon the adhesion of ultrasound contrast agent (UCA) to targeted molecular markers of disease. This is accomplished by coating the surface of the contrast agent with a ligand that specifically binds to the intended molecular marker. Most UCA particles remain in the blood space, and their retention is influenced by the forces imposed by blood flow. For a UCA bound to a molecular target on the vascular endothelium, blood flow imposes a dislodging force that counteracts retention. Additionally, contrast agent adhesion to the molecular marker requires rapid binding kinetics, especially in rapid blood flow. The ability of a ligand:target bond complex to mediate fast adhesion and withstand dislodging force is necessary for efficient ultrasound-based molecular imaging. In the current study, we describe a flow-based adhesion assay which, combined with a novel automated tracking algorithm, enables quick determination of the ability of a targeting ligand to mediate effective contrast agent adhesion. This system was used to explore the adhesion of UCA targeted to the proinflammatory endothelial protein P-selectin via four targeting ligands, which revealed several interesting adhesive behaviors. Contrast agents targeted with glycoconjugate ligands modeled on P-selectin glycoprotein ligand 1 exhibited primarily unstable or transient adhesion, while UCA targeted with an anti-P-selectin monoclonal antibody exhibited primarily firm adhesion, although the efficiency with which these agents were recruited to the target surface was relatively low.

Keywords: Molecular imaging; ultrasound contrast; targeting; P-selectin; flow chamber; glycosulfopeptide

Introduction

Molecular imaging enables detection of phenotypic alterations at the molecular level. This technique provides enormous utility in the context of clinical diagnosis. It is

* Address correspondence to this author. Mailing address: University of Virginia Cardiovascular Division, P.O. Box 800158, Hospital Drive, Cobb Hall, RM 1026, Charlottesville, VA 22908-0158. E-mail: ALK6N@virginia.edu. Tel: (434) 243-9773. Fax: (434) 982-3183.

[†] University of Virginia Department of Biomedical Engineering.
[‡] University of Virginia Department of Electrical and Computer Engineering.
[§] University of Oklahoma Health Sciences Center.
[#] University of Helsinki.
[||] University of Virginia Robert M. Berne Cardiovascular Research Center.
[⊥] University of Virginia Cardiovascular Division.

10.1021/mp0600541 CCC: $33.50
Published on Web 09/15/2006

also a tool for investigation of disease process in a research setting. Most conventional imaging modalities are now capable of performing molecular imaging,[1] although ultrasound offers the unique advantages of real-time imaging, high portability, and relatively low equipment cost and does not require ionizing radiation. Ultrasound-based molecular imaging relies upon the detection of intravascular contrast agents, typically gas-encapsulated microparticles, coated with a targeting ligand specific for the target molecule of interest (reviewed in ref 2). Several ultrasound contrast agent (UCA) formulations can be readily labeled with a wide variety of targeting ligands using simple coupling chemistries. This technique has been used to image pathophysiology in several animal models of disease, including post-ischemic injury,[3] transplant rejection,[4] thrombus,[5−7] tumor angiogenesis,[8,9] inflammatory bowel disease,[10] and autoimmune encephalitis.[11]

Successful use of ultrasound molecular imaging requires careful selection of an appropriate targeting ligand. Four characteristics are necessary in a ligand: specificity, affinity, binding rate, and response to applied force. Monoclonal antibodies have commonly been utilized as targeting ligands, and typically offer optimal specificity to the desired molecular target. Several well-established methods for screening targeting ligands for specificity and affinity are available. Affinity is often determined by radiolabeled ligand binding assays or using the Biacore instrument[12] (surface plasmon resonance). Targeted ultrasound contrast agent must adhere under flow, which requires knowledge of the inherent kinetics of the ligand:target pair, especially on-rate, and understanding how the bond complex behaves under applied force.

Unlike the single-molecule contrast agents used in other molecular imaging modalities, ultrasound contrast agents are particulate, and therefore are subject to viscous drag forces found in the vascular circulation. The dislodging force imposed by blood flow on a microscopic UCA tethered to an endothelial molecular marker is thousands to millions of times greater than that on a single molecule due to the larger size of the UCA. This dislodging force imparts a tensile stress on the ligand:target bond complex,[13] which can influence the stability of the bond.[14,15] The force on a load-bearing ligand:target bond complex is proportional to the local fluid force upon the tethered particle[16] divided by the number of bonds. Insufficient resistance under applied force may limit the ability of a UCA to achieve adhesion to a molecular target in vigorous blood flow.

A bond complex requires a finite amount of time to form at any given local concentration, which is commonly expressed by the molecular on-rate. Successful UCA retention requires that the molecular on-rate be rapid enough for bond formation to occur in the limited time that the individual partnering molecules are in proper contact. For the case of a UCA conveyed across targeted endothelium by the blood flow, rapid bond formation is clearly desirable; successful UCA retention in blood vessels exhibiting rapid blood flow requires rapid bond kinetics. Formation of the initial ligand:target bond is typically termed tethering or capture, and the efficiency with which this occurs is an intrinsic molecular property of the ligand.

(1) Jaffer, F. A.; Weissleder, R. Seeing within: molecular imaging of the cardiovascular system. *Circ. Res.* **2004**, *94*, 433−445.
(2) Lindner, J. R. Microbubbles in medical imaging: current applications and future directions. *Nat. Rev. Drug Discovery* **2004**, *3*, 527−532.
(3) Lindner, J. R.; Song, J.; Xu, F.; Klibanov, A. L.; Singbartl, K.; Ley, K. Noninvasive ultrasound imaging of inflammation using microbubbles targeted to activated leukocytes. *Circulation* **2001**, *102*, 2745−2750.
(4) Weller, G. E. R.; Lu, E.; Csikari, M. M.; Klibanov, A. L.; Fischer, D.; Wagner, W. R.; Villanueva. F. S. Ultrasound imaging of acute cardiac transplant rejection with microbubbles targeted to intercellular adhesion molecule-1. *Circulation* **2003**, *108*, 218−224.
(5) Lanza, G. M.; Wallace, K. D.; Fischer, S. E.; Christy, D. H.; Scott, M. J.; Trousil, R. L.; Cacheris, W. P.; Miller, J. G.; Gaffney, P. J.; Wickline, S. A. High-frequency ultrasonic detection of thrombi with a targeted contrast system. *Ultrasound Med. Biol.* **1997**, *23*, 863−870.
(6) Hamilton, A.; Huang, S. L.; Warnick, D.; Stein, A.; Rabbat, M.; Madhav, T.; Kane, B.; Nagaraj, A.; Klegerman, M.; MacDonald, R.; McPherson, D. Left ventricular thrombus enhancement after intravenous injection of echogenic immunoliposomes: studies in a new experimental model. *Circulation* **2002**, *105*, 2772−2778.
(7) Schumann, P. A.; Christiansen, J. P.; Quigley, R. M.; McCreery, T. P.; Sweitzer, R. H.; Unger, E. C.; Lindner, J. R.; Matsunaga, T. O. Targeted-microbubble binding selectively to GPIIB IIIA receptors of platelet thrombi. *Invest. Radiol.* **2002**, *37*, 587−593.
(8) Ellegala, D. B.; Leong-Poi, H.; Carpenter, J. E.; Klibanov, A. L.; Kaul, S.; Shaffrey, M. E.; Sklenar, J.; Lindner, J. R. Imaging tumor angiogenesis with contrast ultrasound and microbubles targeted to alpha(v) beta3. *Circulation* **2003**, *108*, 336−341.
(9) Weller, G. E. R.; Wong, M. K. K.; Modzelewski, R. A.; Lu, E.; Klibanov, A. L.; Wagner, W. R.; Villanueva, F. S. Ultrasonic imaging of tumor angiogenesis using contrast microbubbles targeted via the tumor-binding peptide arginine-arginine-leucine, *Cancer Res.* **2005**, *65*, 533−539.
(10) Bachmann, C.; Klibanov, A. L.; Olson, T. S.; Sonnenschein, J. R.; Rivera-Nieves, J.; Cominelli, F.; Ley, K. F.; Lindner, J. R.; Pizarro, T. T. Targeting mucosal addressin cellular adhesion molecule (MAdCAM)-1 to noninvasively image experimental Crohn's disease. *Gastroenterology* **2006**, *130*, 8−16.
(11) Linker, R. A.; Reinhardt, M.; Bendszus, M.; Ladewig, G.; Briel, A.; Schirner, M.; Maurer, M.; Hauff, P. In vivo molecular imaging of adhesion molecules in experimental autoimmune encephalomyelitis (EAE). *J. Autoimmun.* **2005**, *25*, 199−205.
(12) Huber, A.; Demartis, S.; Neri, D. The use of biosensor technology for the engineering of antibodies and enzymes. *J. Mol. Recognit.* **1999**, *12* (3), 198−216.
(13) Alon, R.; Hammer, D. A.; Springer, T. A. Lifetime of the P-selectin-carbohydrate bond and its response to tensile force in hydrodynamic flow. *Nature* **1995**, *374*, 539−542.
(14) Rinko, L. J.; Lawrence, M. B.; Guilford, W. H. The molecular mechanics of P- and L-selectin lectin domains binding to PSGL-1. *Biophys. J.* **2004**, *86*, 544−554.
(15) Tees, D. F.; Waugh, R. E.; Hammer, D. A. A microcantilever device to assess the effect of force on the lifetime of selectin-carbohydrate bonds. *Biophys. J.* **2001**, *80*, 668−682.
(16) Smith, M. J.; Berg, E. L.; Lawrence, M. B. A direct comparison of selectin-mediated transient, adhesive events using high temporal resolution. *Biophys. J.* **1999**, *77*, 3371−3383.

Although molecular imaging using targeted UCA has received significant attention, the investigation of biophysical characteristics of targeting ligands has begun only recently. Adhesion molecule biomechanics has been extensively investigated in the context of the leukocyte adhesion cascade (for review, see ref 17). A key tool in this regard is the parallel plate flow chamber, which enables investigation of the role of fluid flow and receptor site density on particle adhesion independent of anatomical features that may confound analysis in vivo.[18,19] Several studies have utilized the flow chamber to explore UCA retention to a target substrate.[6,20,21] In the current study, we have used this technique in conjunction with a computerized automated tracking program to analyze the adhesion of UCA targeted to the proinflammatory molecule P-selectin, and explored the adhesive behavior of four P-selectin-specific targeting ligands. We report that each proposed ligand enables UCA retention to P-selectin with varying efficiency, and that alterations in fluid flow rate and target density result in distinct adhesive behaviors.

Experimental Section

1. Antibodies, Glycoconjugates, and Buffers. The rat monoclonal antibody against murine P-selectin Rb40.34[22] was purified from hybridoma supernatant at the University of Virginia Lymphocyte Culture Center (Charlottesville, VA) and dialyzed overnight against Dulbecco's phosphate-buffered saline (DPBS, Gibco-Invitrogen, Grand Island, NY) using a 10 000 Dalton MWCO dialysis cartridge (Pierce, Rockford, IL). The antibody was biotinylated with *N*-hydroxysuccinimidobiotin (Sigma, St. Louis, MO), followed by overnight dialysis. The chemoenzymatic synthesis and C-terminal biotinylation of the glycoconjugates used in these experiments has been described in depth previously.[23,24] The peptide sequence of these molecules corresponded to amino acids 45−61 of native human PSGL-1. Three glycoconjugates were investigated: (1) 2-GSP-6, which is tyrosine sulfated at residues 46, 48, and 51, bears an O-glycan capped with sLe^x at Thr-57. (2) 2-GP-6 is a glycopeptide bearing the O-glycan but no tyrosine sulfation. (3) 2-GSP-1 is incompletely glycosylated, bearing only a GalNAc at Thr-57 and three tyrosine sulfates. Each of these peptides was biotinylated at a COOH-terminal cysteine. The structure of each of the glycoconjugates is shown in Figure 1. Recombinant murine P-selectin was purchased from R&D Systems (Minneapolis, MN).

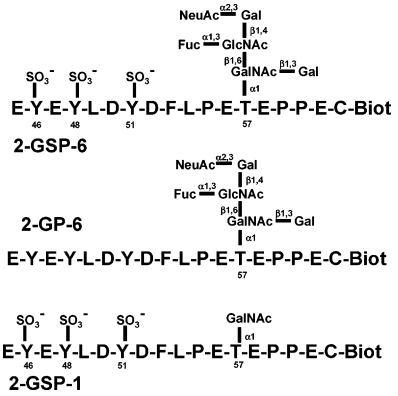

Figure 1. Schematic diagram of glycoconjugates.

2. Targeted Microbubble Preparation. Microbubble UCA preparations used in these experiments were composed of a decafluorobutane (C_4F_{10}) gas core encapsulated by a lipid monolayer shell. A layer of poly(ethylene glycol) (PEG) was grafted onto the lipid shell, and targeting ligands were conjugated to the distal tips of the PEG molecules using biotin−streptavidin coupling chemistry.[3] Briefly, the UCA were incubated with 3 μg of streptavidin per 10^7 particles under C_4F_{10} on ice for 30 min, followed by two centrifugal washes to remove unreacted streptavidin. The UCA were then incubated for 30 min on ice with 10^{-11} mol of biotinylated Rb40.34 or glycoconjugate per 10^7 particles. The UCA was subsequently centrifuged twice and diluted to 5 $\times$ 10^6 particles/mL for adhesion assays. The size distribution of the UCA populations was assessed using electrozone sensing with a Coulter Multisizer IIe (Beckman-Coulter, Miami, FL).

3. P-Selectin Substrate Preparation. Polystyrene dishes 35 mm in diameter (Corning, Corning, NY) were washed with methanol prior to adsorption of P-selectin. P-selectin (25 or 400 ng) was diluted to a final volume of 200 μL in DPBS and incubated in a 1 cm diameter circle at the center of the dish overnight at 4 °C. Dishes were then washed five times with 0.05% Tween-20 (J. T. Baker, Phillipsburg, NJ) and blocked with 2 mL of casein blocker solution (Pierce, Rockford, IL) for at least 2 h at room temperature. The site

(17) Simon, S. I.; Green, C. E. Molecular mechanics and dynamics of leukocyte recruitment during inflammation. *Annu. Rev. Biomed. Eng*. **2006**, *7*, 151−185.

(18) Lawrence, M. B.; McIntire, L. V.; Eskin, S. G. Effect of flow on polymorphonuclear leukocyte/endothelial cell adhesion. *Blood* **1987**, *70*, 1284−1290.

(19) Goetz, D. J.; Greif, D. M.; Shen, J.; Luscinskas, F. W. Cell-cell adhesive interactions in an in vitro flow chamber. *Methods Mol. Biol.* **1999**, *96*, 137−145.

(20) Takalkar, A. M.; Klibanov, A. L.; Rychak, J. J.; Lindner, J. R.; Ley, K. Binding and detachment dynamics of microbubbles targeted to P-selectin under controlled shear flow. *J. Controlled Release* **2004**, *96*, 473−482.

(21) Weller, G. E. R.; Villanueva, F. S.; Tom, E. M.; Wagner, W. M. Targeted ultrasound contrast agents: in vitro assessment of endothelial dysfunction and multi-targeting to ICAM-1 and Sialyl Lewis^x. *Biotechnol. Bioeng.* **2005**, *92*, 780−788.

(22) Bosse, R.; Vestweber, D. Only simultaneous blocking of the L- and P-selectin completely inhibits neutrophil migration into mouse peritoneum. *Eur. J. Immunol*. **1994**, *24*, 3019−3024.

(23) Leppänen, A.; Mehta, P.; Ouyang, Y. B.; Ju, T.; Helin, J.; Moore, K. L.; van Die, I.; Canfield, W. M.; McEver, R. P.; Cummings, R. D. A novel glycosulfopeptide binds to P-selectin and inhibits leukocyte adhesion to P-selectin. *J. Biol. Chem*. **1999**, *274*, 24838−2448.

(24) Leppänen, A.; White, S. P.; Helin, J.; McEver, R. P.; Cummings, R. D. Binding of glycosulfopeptides to P-selectin requires stereospecific contributions of individual tyrosine sulfate and sugar residues. *J. Biol. Chem.* **2000**, *275*, 39569−39578.

density of P-selectin on the polystyrene dishes was determined using time-resolved fluorometric detection of Eu-labeled streptavidin.[20] The lower and higher incubation concentration resulted in P-selectin surface densities of 7 and 140 molecules/μm^2, respectively. Control dishes were blocked with casein alone.

4. Laminar Flow Assay. The inverted parallel plate flow chamber used in the in vitro adhesion experiments has been described earlier.[20] P-selectin coated dishes were placed in the flow chamber deck (GlycoTech, Rockville, MD), and the flow chamber was inverted with a specially fabricated holder. Flow through the chamber was controlled with a syringe pump operating in the withdrawal mode (Harvard Apparatus, Cambridge, MA). The flow chamber was mounted on the stage of an inverted microscope (Laborlux 11; Leitz, Rockleigh, NJ) equipped with a 40× objective. Videomicroscopic data was recorded with a CCD camera (GE Interlogix, Corvallis, OR) operating at 30 frames/s onto MiniDV (Sony, Tokyo, Japan) digital videocassettes.

Contrast agents (5×10^6 particles/mL) were dispersed in DPBS containing 1.0 mM Ca^{2+} and infused into the flow chamber at a wall shear stress of 0.7, 1.7, 3.1, or 4.5 dyn/cm^2. Wall shear stress was calculated from the volumetric flow rate (Q), controlled by the syringe pump, as

$$\tau = \frac{6Q}{h^2 w} \tag{1}$$

where h is the height of the flow path (0.0127 cm) and w is the width of the flow path (0.25 cm). Four flow chambers were analyzed at each wall shear stress for each UCA formulation. The UCA dispersion was continuously stirred with a magnetic stir bar throughout each experiment to ensure uniform concentration. Contrast agent adhesion was observed for 30 s in a single field of view (110 μm × 150 μm) near the center of the dish for each experiment. Videomicroscopic data were exported from digital video cassette to an Apple iBook G4 running iMovie (v. 3.0.3; Apple, Cupertino, CA) at a spatial resolution of 0.22 μm per pixel. Individual experiments were converted to separate audio−video interlaced (avi) files using iMovie prior to tracking.

5. Automated Tracking. Contrast agent adhesion was quantified using a MATLAB-based automated tracking algorithm.[25] Videomicroscopic data, in the form of AVI files, were first processed using morphological filters to detect UCA particles (based on size and intensity) against the background. On the basis of those detection results, the algorithm tracks all UCA particles using a Bayesian statistical method. Additional processes to detect merger (two overlapping MB detected as one) and to exclude false-positive correlations were also applied. The flux of free-stream (noninteracting) particles traversing across the target surface was detected as the average number of discrete particles that cross a set of randomly placed vertical thresholds in each field of view. A correction factor was derived to account for particles translating far from the target surface. The software produced a series of bitmaps in which each tracked particle is assigned a number, a position-versus-time plot of each particle, and a spreadsheet containing the instantaneous x- and y-position and size of each particle.

Slight variations in the intensity of the detected particle can result in noise in the position−time data. To account for this, the position−time data produced from the autotracker were filtered using a spreadsheet template (Microsoft Excel, v. 11.1). The filter assigned motion in the negative direction (opposite the direction of flow) a velocity of zero, and eliminated particle "jitter".

6. Data Analysis. Instantaneous microbubble velocity was calculated frame-by-frame from the position data. Particle capture was defined as the instant in which the velocity of a particle first dropped below 50% of the hydrodynamic velocity (U_h), calculated according to[26]

$$U_h = h \cdot \gamma \left[1 - \frac{5}{16}\left(\frac{a}{h}\right)^3\right] \tag{2}$$

where a is the particle radius (μm), ($h + a$) is the distance from the center of the particle to the target surface (h was set at 100 nm for all experiments), and γ is the fluid shear rate (s^{-1}) in the absence of a particle. Only particles that interact with the target surface for at least 10 frames (0.33 s) were scored as captured; very short duration adhesive events were not analyzed. The ability of a ligand to mediate UCA capture was expressed as capture efficiency, defined as the ratio of capture events divided by the number of free-stream UCA that entered the field of view. Normalization of capture frequency by free-stream flux accounted for variation in UCA delivery to the target surface with fluid flow rate.[27]

Adhesive interactions between UCA and the target surface were classified as rolling or firm adhesion. Firm adhesion was defined as a translational velocity equal to zero for a duration of at least 5 s. Rolling was defined as a translational velocity below 50% of U_h. Detachment occurred when a firmly adherent UCA achieved a velocity greater than 50% of U_h after capture. No detachment directly from rolling was observed; that is, rolling UCA either persisted in rolling for the duration of the experiment or achieved firm adhesion.

Two parameters representing the ability of a targeting ligand to convert capture events into firm adhesion were examined. The firm adhesion fraction was computed as the frequency of UCA firm adhesion (number of firmly adherent particles per time) relative to the capture frequency (number of captured particles per time); firm adhesion fraction

(25) Li, B.; Tay, P. C.; Acton, S. T. Multi-assignment interacting multiple model for tracking microbubbles. Presented at the Annual Asilomar Conference on Signals, Systems and Computers, Pacific Grove, CA, 2005.

(26) Goldman, A. J.; Cox, R. G.; Brenner H. Slow viscous motion of a sphere parallel to a plane wall - II Couette flow. *Chem. Eng. Sci.* **1967**, *22*, 653−660.

(27) Munn, L. L.; Melder, R. J.; Jain, R. K. Analysis of cell flux in the parallel plate flow chamber: implications for cell capture studies. *Biophys. J.* **1994**, *67*, 889−895.

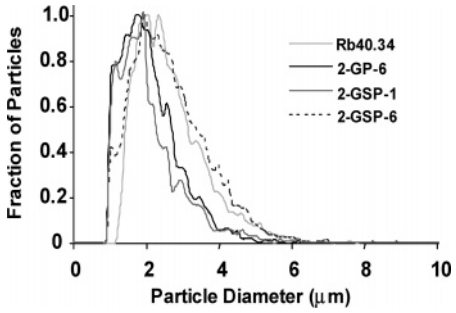

Figure 2. Size distribution of targeted UCA. Distributions were assessed using electrozone sensing. The median diameters of all UCA preparations were statistically identical.

Table 1. Mean Diameter of Ultrasound Contrast Agent Particles

WSS (dyn/cm^2)	RB40.34	2-GP-6	2-GSP-1	2-GSP-6
4.5	1.31 ± 0.04	1.42 ± 0.07	1.54 ± 0.06	1.49 ± 0.08
3.1	1.57 ± 0.10	1.44 ± 0.05	1.36 ± 0.06	1.34 ± 0.06
1.7	1.50 ± 0.03	1.40 ± 0.07	1.29 ± 0.04	1.55 ± 0.05
0.7	1.51 ± 0.02	1.49 ± 0.04	1.43 ± 0.03	1.55 ± 0.05

represents the efficiency with which a ligand enables firm adhesion subsequent to capture. Only captured particles were analyzed; particles that rolled into the field of view or were already present were excluded. The detachment fraction was similarly computed as the frequency of detachment relative to the capture frequency. Rolling adhesion was examined in terms of the rolling velocity, defined as mean translational velocity of a rolling UCA over the duration of tracking (5−25 s).

Capture efficiency was expressed as mean ± SEM for four flow chamber experiments. Mean rolling velocity was expressed as the overall mean ± SEM of all analyzed particles. The statistical significance of differences in capture efficiency among the four ligands was determined using one-way ANOVA with Tukey's comparison, as appropriate. Differences in capture efficiency between each ligand with wall shear stress and P-selectin site density were tested using two-way ANOVA.

Results

1. Microbubble Characterization. The size distribution of preparations of UCA bearing each of the four targeting ligands is shown in Figure 2. The median diameter of the UCA targeted with 2-GSP-6, 2-GP-6, 2-GSP-1, and Rb40.34 was 2.4 ± 0.2, 2.5 ± 0.2, 2.4 ± 0.2, and 2.2 ± 0.4 μm, respectively. There was no difference in the mean or median diameter between the preparations.

The diameter of each particle that interacted with the target surface was measured using the automated tracking program. The mean diameter of interacting particles on 7 sites/μm^2 P-selectin is presented in Table 1. There was no difference in the mean diameter of interacting particles at each wall shear stress on either 7 or 140 sites/μm^2 of P-selectin.

2. Autotracker Validation. The flux (particles/minute) of non-interacting UCA across the field of view was

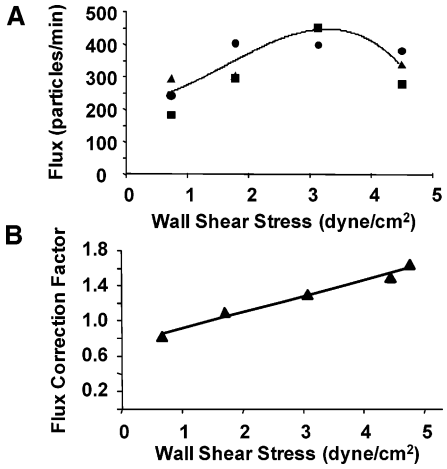

Figure 3. Derivation of flux correction factor. (A) Hand-tracked particle flux at four wall shear stresses for $n = 3$ flow chambers. Symbols (square, circle, triangle) represent mean flux from single flow chamber. Line represents third-order polynomial best fit ($R^2 = 1$). (B) Flux correction factor (symbols). Line represents linear fit ($R^2 = 0.98$).

determined using the automated tracking program. The accuracy of this flux measurement was assessed by comparison with hand-tracked flux in three flow chambers at each of four wall shear stresses (Figure 3A). The automated tracker was found to underestimate true flux above ~2 dyn/cm^2; this was due to the distortion in the recorded image of the most rapidly moving particles and shadowing from particles beyond the focal distance. A flux correction factor, defined as the quotient of the true flux and tracked flux, was calculated for each examined WSS (Figure 3B). In all experiments, tracked flux was multiplied by the appropriate flux correction factor to produce the true flux. Characteristic videomicroscopic and autotracked images are shown in Figure 4A and Figure 4B, respectively.

3. Contrast Agent Capture Efficiency. Capture efficiency represents the ability of the ligand to initiate adhesion of a moving UCA to the target surface. Capture efficiency decreased with wall shear stress on 7 sites/μm^2 for 2-GSP-1; wall shear stress did not influence the capture efficiency of the other three ligands. A statistically significant dependence of capture efficiency on P-selectin site density was observed for 2-GSP-1 and 2-GSP-6. Capture efficiency of 2-GSP-1 was significantly greater on the higher P-selectin site density than the lower, while capture efficiency of 2-GSP-6 was observed to be higher on the lower site density (Figure 5).

The capture efficiency of 2-GSP-6 was significantly greater than that of the other ligands on 7 sites/μm^2 P-selectin. Capture efficiencies of 2-GSP-6 and 2-GSP-1 were similar on 140 sites/μm^2, and both were significantly higher than those of Rb40.34 and 2-GP-6 at all wall shear stresses except 4.5 dyn/cm^2.

4. Fraction of Adherent and Detached Contrast Agents. A summary of the observed adhesive behaviors is given in Figure 6. Almost all UCA coated with the anti-P-selectin

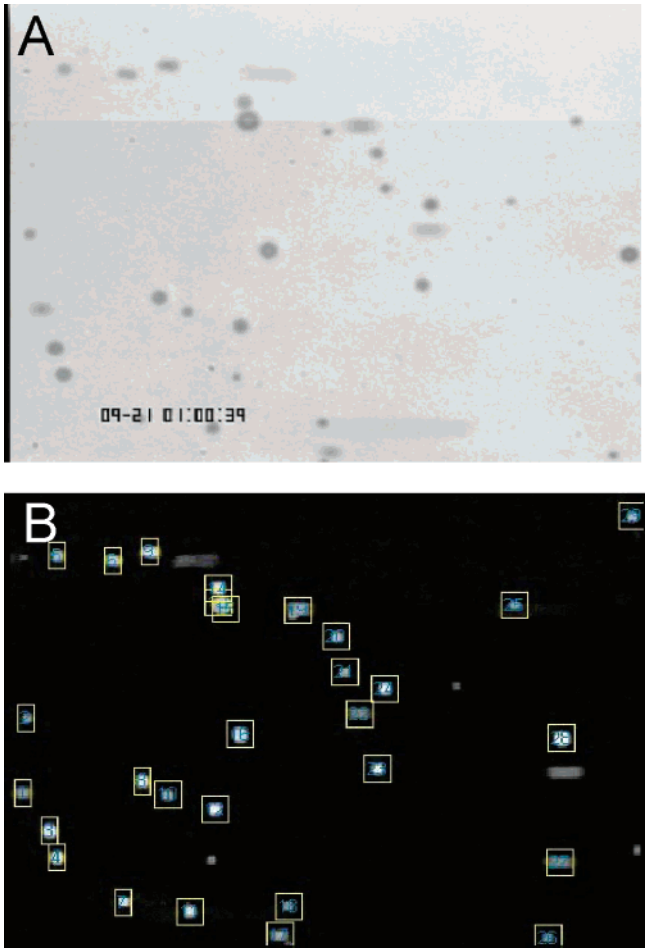

Figure 4. Automated tracking results. (A) Characteristic video microscopic image of UCA traversing the target surface. (B) Automated tracking image after particle detection and background subtraction. Tracked particles are identified by enumerated boxes.

mAb Rb40.34 attached firmly. No rolling and relatively infrequent detachment of these UCA was observed. The fraction of captured 2-GSP-1 and 2-GP-6 targeted UCA that achieved firm adhesion was uniformly low under all conditions; the majority of these UCA proceeded to rolling adhesion after capture. However, detachment of 2-GSP-1 targeted UCA was frequently observed, predominantly on the lower P-selectin site density, while detachment of 2-GP-6 targeted UCA was not observed under any conditions. UCA targeted with 2-GSP-6 exhibited interesting site-dependent behavior: almost no firm adhesion was observed on 7 sites/μm^2 of P-selectin, and the majority of captured UCA proceeded to rolling adhesion. On 140 sites/μm^2, most captured UCA became firmly adherent at wall shear stresses below 3.1 dyn/cm^2, above which rolling adhesion predominated.

5. Contrast Agent Rolling Velocity. Contrast agent rolling velocity is shown in Figure 7. The rolling velocity of UCA targeted with 2-GP-6 and 2-GSP-1 was relatively invariant with wall shear stress on 7 and 140 sites/μm^2 of P-selectin. On 7 sites/μm^2, the rolling velocity of 2-GSP-6 increased with wall shear stress, while rolling was not

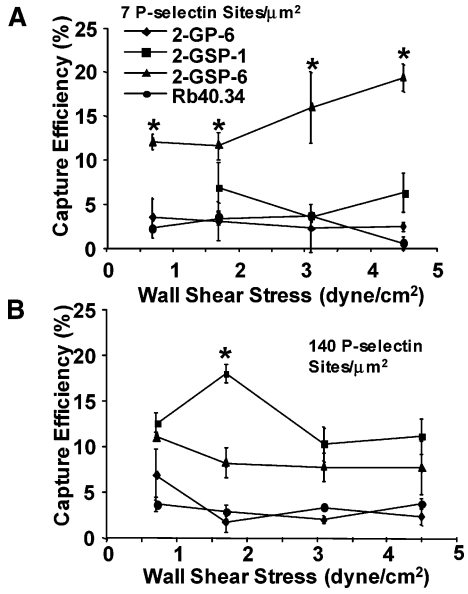

Figure 5. Contrast agent capture efficiency on (A) 7 sites/μm^2 and (B) 140 sites/μm^2 P-selectin. Mean of four flow chambers $\pm$ SEM. An asterisk (*) represents $p < 0.05$ between all other conditions at the same wall shear stress.

observed on 140 sites/μm^2. No rolling of UCA targeted with Rb40.34 was observed.

Discussion

In the current study we have used automated tracking of UCA adhesion in a flow chamber to explore the adhesive behavior of P-selectin-binding targeting ligands. We examined three criteria by which a molecule may be judged a suitable ligand for targeted ultrasound-based molecular imaging: the ability of a ligand to mediate capture of a circulating UCA to the target surface, a ligand's ability to mediate firm (as opposed to transient) adhesion, and resistance to detachment. Use of the method described here has allowed us to explore the suitability of the screened ligands, and elucidated several interesting adhesive behaviors.

The glycoconjugate ligands examined here were modeled on the P-selectin binding region of the leukocyte adhesion molecule PSGL-1.[28] Several studies have confirmed this molecule's ability to mediate adhesion of cells and microspheres to P-selectin in vitro[29] and in vivo.[30,31] The presence of both tyrosine sulfation and a core-2 O-glycan are required for PSGL-1 to mediate high-affinity binding to P-selectin,[23] although the tetrasaccharide sialyl Lewis^x (sLe^x) alone has

(28) Liu, W.; Ramachandran, V.; Kang, J.; Kishimoto, T. K.; Cummings, R. D.; McEver, R. P. Identification of N-terminal residues on P-selectin glycoprotein ligand-1 required for binding to P-selectin. *J. Biol. Chem.* **1998**, *273*, 7078−7087.

(29) Patil, V. R. S.; Campbell, C. J.; Yun, Y. H.; Slack, S. M.; Goetz, D. J. Particle diameter influences adhesion under flow. *Biophys. J.* **2001**, *80*, 1733−1743.

(30) Norman, K. E.; Katopodis, A. G.; Thoma, G.; Kolbinger, F.; Hicks, A. E.; Cotter, M. J.; Pockley, A. G.; Hellewell, P. G. P-selectin glycoprotein ligand-1 supports rolling on E- and P-selectin in vivo. *Blood* **2000**, *96*, 3585−3591.

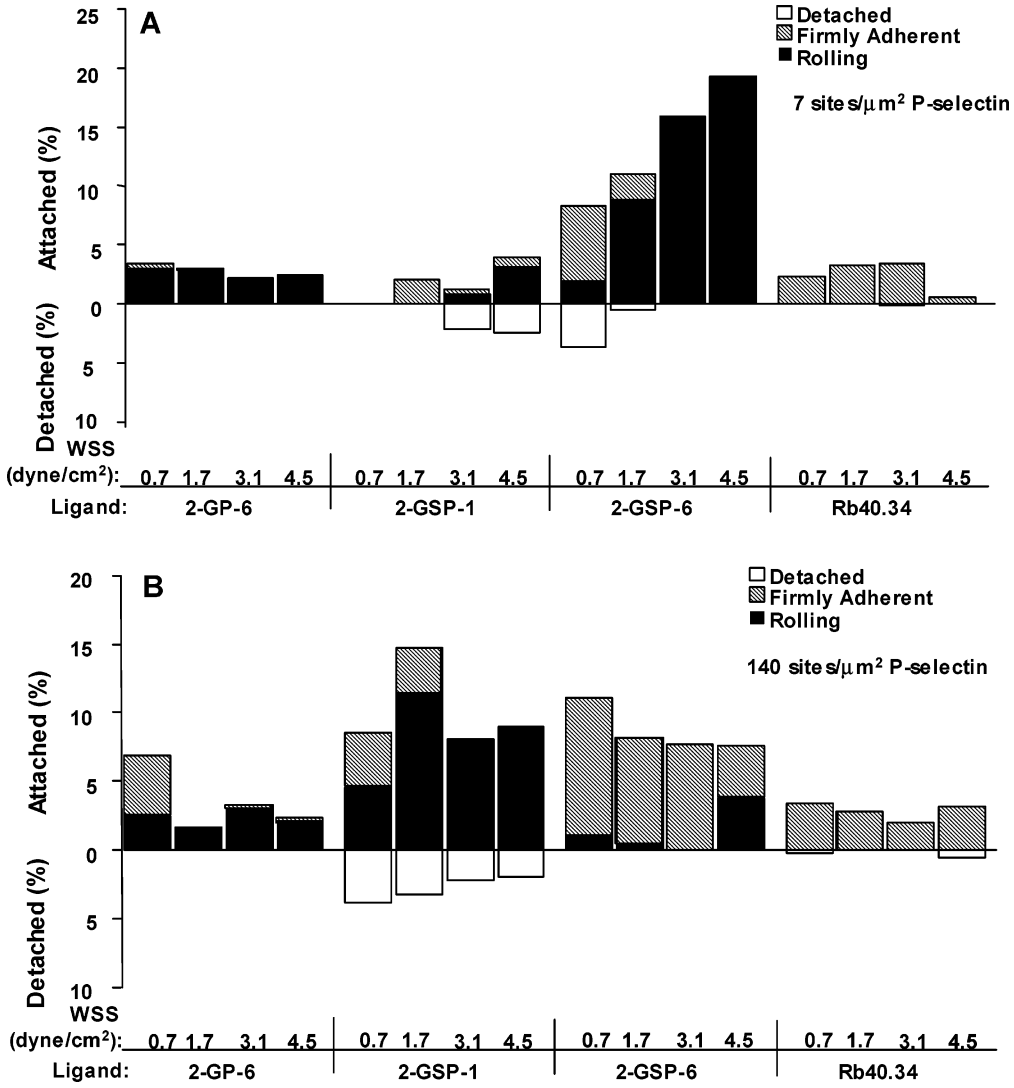

Figure 6. Contrast agent adhesive interactions on (A) 7 sites/μm^2 and (B) 140 sites/μm^2 P-selectin. Bars represent the fraction of the captured UCA that became firmly adherent, detached, or rolled without detachment or firm adhesion.

been shown to mediate limited adhesion of microspheres,[32,33] model drug delivery vehicles[34] and ultrasound contrast agents[21] to P-selectin and E-selectin. Interestingly, we observed that each of the glycoconjugates examined here could mediate capture of UCA to P-selectin, with an efficiency equivalent to or surpassing that of the monoclonal antibody Rb40.34 under most conditions.

Our data revealed that 2-GSP-6, which contains both tyrosine sulfation and complete glycosylation, mediates UCA capture to P-selectin 3−5 times more efficiently than the other ligands. The incompletely glycosylated 2-GSP-1 mediated high-efficiency capture only on the high P-selectin site density, although this adhesion was unstable and resulted in UCA detachment. The monoclonal antibody Rb40.34 and the nonsulfated 2-GP-6 mediated capture at an efficiency of ~5% or lower under most conditions examined here. Nearly all of the UCA targeted with Rb40.34 that were captured proceeded to firm adhesion, although some detachment was observed at the highest wall shear stress. This contrasts strikingly with the behavior of the glycoconjugates, which mediated primarily rolling adhesion subsequent to capture. Notably, UCA targeted with 2-GSP-6 did exhibit firm adhesion on 140 sites/μm^2 of P-selectin, but not on 7 sites/μm^2. Our data suggests that 2-GSP-6 can mediate high-efficiency capture of UCA under all conditions examined, although captured UCA do not necessarily achieve firm adhesion. Rb40.34, in contrast, mediates UCA capture with

(31) Burch, E. E.; Shinde Patil, V. R.; Camphausen, R. T.; Kiani, M. F.; Goetz, D. J. The N-terminal peptide of PSGL-1 can mediate adhesion to trauma-activated endothelium via P-selectin in vivo. *Blood* **2002**, *100*, 531−538.

(32) Rodgers, S. D.; Camphausen, R. T.; Hammer, D. A. Sialys Lewis^x-mediated, PSGL-1-independent rolling adhesion on P-selectin. *Biophys. J.* **2000**, *79*, 695−706.

(33) Yago, T.; Leppänen, A.; Qiu, H.; Marcus, W. D.; Nollert, M. U.; Zhu, C.; Cummings, R. D.; McEver, R. P. Distinct molecular and cellular contributions to stabilizing selectin-mediated rolling under flow. *J. Cell Biol.* **2002**, *158*, 787−799.

(34) Eniola, A. O.; Rodgers, S. D.; Hammer, D. A. Characterization of biodegradable drug delivery vehicles with the adhesive properties of leukocytes. *Biomaterials* **2002**, *23*, 2167−2177.

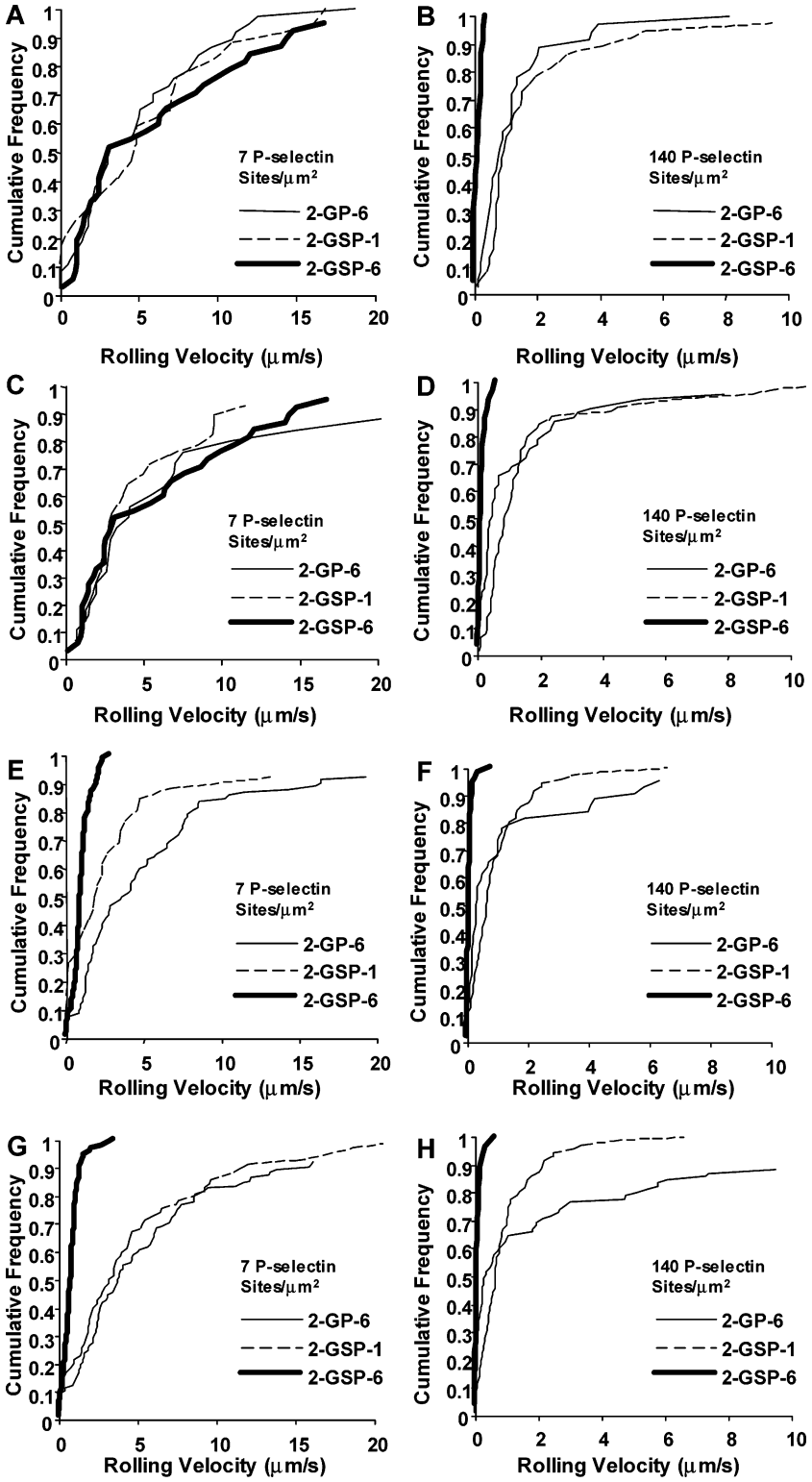

Figure 7. Contrast agent cumulative rolling velocity. Rolling velocities of UCA targeted with glycoconjugates at 0.7 dyn/cm^2 on (A) 7 sites/μm^2 and (B) 140 sites/μm^2 P-selectin; at 1.7 dyn/cm^2 on (C) 7 sites/μm^2 and (D) 140 sites/μm^2 P-selectin; at 3.1 dyn/cm^2 on (E) 7 sites/μm^2 and (F) 140 sites/μm^2 P-selectin; at 4.5 dyn/cm^2 on (G) 7 sites/μm^2 and (H) 140 sites/μm^2 P-selectin.

significantly lower efficiency, although captured UCA tend to remain firmly adherent.

High capture efficiency and the ability to mediate effective firm adhesion are desirable qualities in a targeting ligand. Of the four ligands examined here, only 2-GSP-6 appears to possess both qualities, although firm adhesion efficiency with this ligand was dependent upon target site density. This suggests that 2-GSP-6 may be a useful targeting ligand for imaging inflammation. However, as pointed out by Weller and colleagues,[21] the ability to detect the disease along a

continuum of severity is a necessary ability for effective molecular imaging. The inability of 2-GSP-6 to mediate firm adhesion on low P-selectin site density may obviate its use as a robust targeting ligand, although the rolling velocity of UCA targeted with this ligand was on the order of several micrometers per second, corresponding to a relatively small distance traveled on the time scale of a typical ultrasound imaging exam. The findings presented here thus illustrate the necessity of careful screening of the adhesive characteristics of a proposed targeting ligand.

Limitations of the current study are related to inherent limitations of the flow chamber system. We have identified target site density and fluid wall shear stress as two key determinants of the ability of a UCA to achieve targeted adhesion. The parallel plate flow chamber allows us to manipulate each of these variables independently; however, the flow chamber does not capture the complexity of the in vivo situation. Factors such as varying vessel diameter, non-Newtonian hemodynamics, heterogeneous endothelial surface topography, and vascular geometry are clearly not reproduced in this model system. Additionally, the particular design of the parallel plate flow chamber used in this study permitted investigation of UCA adhesion over a relatively limited range of wall shear stress. Alternative flow chamber designs, such as the microcapillary flow chamber,[35] may allow assessment of UCA adhesion over a wider range of wall shear stress. It should be noted, however, that most previous studies[9,10,20] examined UCA adhesion at relatively low (1−3 dyn/cm^2) wall shear stresses; the results presented here expand the range of shear conditions to elucidate adhesive behavior in more detail. We have not explicitly examined the dependence of UCA retention on administered UCA concentration. Presumably, increasing the administered dose of UCA would result in an increasing number of retained UCA, and ultrasound-based molecular imaging relies upon the assumption of a linear or otherwise known change in acoustic signal with adherent UCA concentration. Optimal dosing requires a balance between acoustic signal and maintenance of vascular homeostasis; additionally, discrimination between adherent UCA and freely circulating UCA is desirable. Recent in vitro studies have suggested that the detection threshold for the microbubble UCA used in this study may be as low as a single microbubble.[36]

Previous studies with Rb40.34-targeted UCA in our lab revealed a density of ~2500 molecules/μm^2 on the surface of the UCA, indicating nearly full coverage of the particle surface;[20] the packing density of the glycosulfopeptides, which are significantly smaller (molecular weight ~4 kDa) than the monoclonal antibody, is on the order of 6×10^5 molecules/μm^2.[37] Therefore, the density of P-selectin on the dish and not the ligand density on the UCA surface is the rate-limiting density in our experiment. Finally, we examined only adhesive events enduring for 10 frames or more. Previous work from our group has described a significant population of very rapid detachment events in Rb40.34-targeted UCA,[38] which are not readily detected by the automated tracking program implemented here.

The complimentary adhesive characteristics of Rb40.34 and 2-GSP-6 suggest a novel targeting strategy in which high efficiency capture and firm adhesion may be achieved by targeting with both targeting ligands. This dual-targeting paradigm has been hypothesized to underlie leukocyte adhesion to inflamed endothelium, a process that utilizes distinct ligands that mediate capture (such as PSGL-1 and L-selectin) and firm adhesion (primarily the β2 integrins) on the surface of the leukocyte.[39] Work from Hammer's group[40] in particular has demonstrated this process in a model polystyrene beads system, and both Weller and colleagues[21] and we[37] have shown enhanced adhesion of UCA targeted with two ligands. The present work identifies candidate ligands for such designs. Flow chamber based characterization of the kinetic properties of targeted UCA is useful for optimization of UCA adhesion to targeted molecular markers, to achieve robust and effective ultrasound-based molecular imaging.

Abbreviations Used

UCA, ultrasound contrast agent; DPBS, Dulbecco's phosphate-buffered saline; GSP, glycosulfopeptide; PSGL-1, P-selectin glycoprotein ligand 1.

Acknowledgment. This work was supported in part by NIH BRP EB 02185 to K.L. A.L.K. is grateful to UVA Cardiovascular Division and Robert M. Berne Cardiovascular Research Center for help and support. A generous donation of laboratory equipment to A.L.K.'s laboratory at UVA Cardiovascular Division by Mallinckrodt Inc. (St. Louis, MO) is appreciated. J.J.R. was supported via NIH Cardiovascular training grant HL07284 to UVA.

MP0600541

(35) Chesnutt, B. C.; Smith, D. F.; Raffler, N. A.; Smith, M. L.; White, E. J.; Ley, K. Induction of LFA-1-dependent neutrophil rolling on ICAM-1 by engagement of E-selectin. *Microcirculation* **2006**, *13*, 99−109.

(36) Klibanov, A. L.; Rasche, P. T.; Hughes, M. S.; Wojdyla, J. K.; Galen, K. P.; Wible, J. H.; Brandenburger, G. H. Detection of individual microbubbles of ultrasound contrast agents - Imaging of free-floating and targeted bubbles. *Invest. Radiol.* **2004**, *39*, 187−195.

(37) Rychak, J. J.; Klibanov, A. L.; Li, B.; Acton, S.; Leppänen, A.; Cummings, R. D.; Ley, K. *Enhanced Microbubble Adhesion to P-selectin with a Physiologically-tuned Targeting Ligand*; Biomedical Engineering Society: Philadelphia, PA, October 2004.

(38) Rychak, J. J.; Lindner, J. R.; Ley, K.; Klibanov, A. L. Deformable gas-filled microbubbles targeted to P-selectin. *J. Controlled Release*, in press.

(39) Smith, C. W. Possible steps involved in the transition to stationary adhesion of rolling neutrophils: a brief review. *Microcirculation* **2000**, *7*, 385−394.

(40) Eniola, A. O.; Wilcox, P. J.; Hammer, D. A. Interplay between rolling and firm adhesion elucidated with a cell-free system engineered with two distinct receptor−ligand pairs. *Biophys. J.* **2003**, *85*, 2720−2731.